A New Type of Manganese Oxide ($MnO_2 \cdot 0.5H_2O$) Derived from $Li_{1.6}Mn_{1.6}O_4$ and Its Lithium Ion-Sieve Properties

Ramesh Chitrakar,† Hirofumi Kanoh,*,† Yoshitaka Miyai, and Kenta Ooi*,†

Shikoku National Industrial Research Institute, 2217-14 Hayashi-cho, Takamatsu 761-0395, Japan

Received January 11, 2000. Revised Manuscript Received July 10, 2000

A new type of adsorbent, $MnO_2 \cdot 0.5H_2O$, was synthesized from $Li_{1.6}Mn_{1.6}O_4$ followed by acid treatment. The hydrothermal reaction of monoclinic type γ-MnOOH with LiOH solution at 120 °C resulted in a H^+/Li^+ ion exchange, giving orthorhombic $LiMnO_2$. The orthorhombic $LiMnO_2$ was transformed to cubic $Li_{1.6}Mn_{1.6}O_4$ ($Li_2Mn_2O_5$) at a temperature higher than 400 °C. The conversion of $Li_{1.6}Mn_{1.6}O_4$ to $MnO_2 \cdot 0.5H_2O$ by acid treatment resulted in contraction of the lattice constant a_0 from 8.14 to 8.05 Å with little dissolution of manganese. The new adsorbent showed a markedly high ion-exchange capacity (7.5 mmol/g) for lithium ions due to its ion-sieve property. The pH titration study suggested the formation of large numbers of uniform sorption sites having relatively high acidity. The uptake of Li^+ ions from lithium-enriched seawater was found to be 5.3 mmol/g (37 mg/g), which is the maximum among the adsorbents studied to date.

Introduction

Lithium manganese oxides are interesting materials. Many lithium manganese oxides and their lithium extraction/insertion reactions have been studied for development of selective adsorbents and cathode materials for rechargeable batteries.[1−20] Because manganese takes both the trivalent and tetravalent states and lithium content varies widely, we can obtain various kinds of lithium manganese oxides. Gummow et al.[9] summarized the ternary Li−Mn−O phase diagram for understanding the relationship between the structure and the discharge/charge behaviors of lithium manganese oxides. Building on their work, we have constructed a phase diagram containing additional proton-type manganese oxides, as a function of manganese valence and Li/Mn and H/Mn mole ratios, as shown in Figure 1. The vertical plane, where the valence of manganese changes but the protons contained do not, is designated the redox region. The horizontal plane, where the valence of manganese does not change but lithium and proton contents vary, is designated the ion-exchange region.

We have studied the lithium extraction/insertion reactions of $LiMn_2O_4$,[6] $Li_{1.33}Mn_{1.67}O_4$,[6] $LiMnO_2$,[13] and Li_2MnO_3[21] in the aqueous phase. The reactions can be classified as redox, ion-exchange, and dissolution types. Most effort has been focused on the spinel-type manganese oxides $LiMn_2O_4$ and $Li_{1.33}Mn_{1.67}O_4$ because they show both the redox-type and ion-exchange-type reactions while having the same spinel structure. $LiMn_2O_4$ has a structure with lithium at the tetrahedral sites and trivalent and tetravalent manganese at the octahedral sites of a cubic close-packed oxygen framework. Progressive extraction of lithium is accompanied by the oxidation of manganese to eventually form λ-MnO_2, which has vacant tetrahedral sites with only tetravalent manganese.[3] Displacement of manganese by lithium may occur until $Li_{1.33}Mn_{1.67}O_4$ is formed with 100% tetravalent manganese.[6] Extraction of lithium from this material progresses mainly by lithium ion-proton exchange to give a spinel-type manganese oxide with lattice protons. The chemical composition is given as $MnO_2 \cdot 0.31H_2O$ because of a small dissolution reaction. The spinel-type manganese oxide $MnO_2 \cdot 0.31H_2O$ is

* To whom correspondence should be addressed.
† E-mail: chitrak@sniri.go.jp; kano@sniri.go.jp; ooi@sniri.go.jp.

(1) Leont'eva, G. V.; Vol'khim, V. V. *Zh. Prikl. Khim*. **1971**, *44*, 2651.
(2) Vol'khim, V. V.; Leont'eva, G. V.; Onorin, S. A. *Neorg. Mater*. **1973**, *9*, 1041.
(3) Hunter, J. C. *J. Solid State Chem*. **1981**, *39*, 142.
(4) Abe, M.; Tsuji, M. *Solv. Extr. Ion Exch*. **1984**, *2*, 253.
(5) Shen, X. M.; Clearfield, A. *J. Solid State Chem*. **1986**, *64*, 270.
(6) Feng, Q.; Miyai, Y.; Kanoh, H.; Ooi, K. *Langmuir* **1992**, *8*, 1861.
(7) Ooi, K.; Miyai, Y.; Katoh, S.; Maeda, H.; Abe, M. *Langmuir* **1990**, *6*, 289.
(8) Kanoh, H.; Ooi, K.; Miyai, Y.; Katoh, S. *Langmuir* **1991**, *7*, 1841.
(9) Gummow, R. J.; Thackeray, M. M. *J. Electrochem. Soc*. **1994**, *141*, 1178.
(10) Ammundsen, B.; Jones, D. J.; Roziere, J.; Burns, G. R. *Chem. Mater*. **1995**, *7*, 2151.
(11) Koetschau, I.; Richard, M. N.; Dahn, J. R. *J. Electrochem. Soc*. **1993**, *142*, 2906.
(12) Amstrong, A. R.; Bruce, P. G. *Nature* **1996**, *381*, 499.
(13) Tang, W.; Kanoh, H.; Ooi, K. *J. Solid State Chem*. **1999**, *142*, 19.
(14) Goodenough, J. B.; Thackeray, M. M.; David, W. I. E.; Bruce, P. G. *Rev. Chim. Miner*. **1994**, *21*, 435.
(15) Thackeray, M. M.; Kock, A. de; Rossouw, M. H.; Liles, D. C.; Brittin R.; Hoge, D. *J. Electrochem. Soc*. **1992**, *139*, 363.
(16) Ohzuku, T.; Ueda, A.; Hirai, T. *Chem. Express* **1992**, *7*, 193.
(17) Guyomard, D.; Tarascon, J. M. *J. Electrochem. Soc*. **1992**, *139*, 937.
(18) Thackeray, M. M. *J. Electrochem. Soc*. **1995**, *142*, 2568.
(19) Reimers, J. N.; Fuller, E. W.; Rossen, E.; Dahn, J. R. *J. Electrochem. Soc*. **1993**, *140*, 3396.
(20) Paulsen, J. M.; Dahn, J. R. *Chem. Mater*. **1999**, *11*, 3065.
(21) Tang, W.; Kanoh, H.; Liu, Z.; Yang, X.; Ooi, K. *Advanced Materials Development & Performance*, Proceedings of the Second International Conference on Advanced Materials Development and Performance Evaluation and Application, Tokushima, Japan, 1999; Vol. 1, p 408.

10.1021/cm0000191 CCC: $19.00
Published on Web 09/23/2000

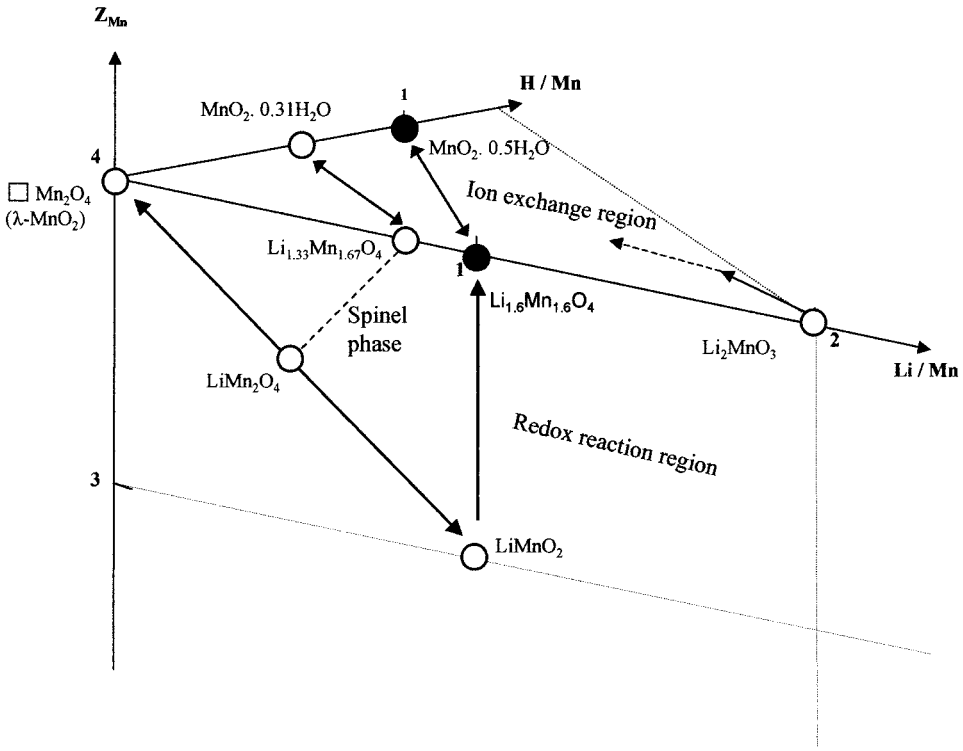

Figure 1. Phase diagram of lithium manganese oxides and their delithiated products.

suitable as a lithium-selective adsorbent because it has a high chemical stability against lithium insertion−extraction in the aqueous phase as well as selective lithium uptake.[22,23] The structural characteristics of $Li_{1.33}Mn_{1.67}O_4$ and its lithium extraction/insertion reactions have been extensively studied by several research groups.[6,10,24−27] A pH titration study has shown that the proton-type sample has a lithium-sieve property and has a high lithium uptake from seawater or brine.[22,23] From neutron diffraction analysis, Ammundsen et al.[24] have concluded that the protons are at the 96g sites, not at the 8a and 16 sites where lithium ions were present, and the tetrahedral sites can reabsorb lithium ions but octahedral sites cannot.

We are interested in $Li_{1.6}Mn_{1.6}O_4$ ($Li_2Mn_2O_5$) as a candidate precursor for a superior lithium-selective adsorbent. We can expect several advantages from this material. First, the ion-exchange capacity may be markedly larger than that of the other manganese oxides because the theoretical exchange capacity reaches 10.5 mmol/g on the basis of the chemical composition. Second, the chemical stability may be sufficiently high because it contains only tetravalent manganese. However, $Li_{1.6}Mn_{1.6}O_4$ can be obtained only by limited methods; it cannot be obtained by conventional solid-phase reaction by heating a mixture of manganese and lithium compounds. It has been obtained by the heat treatment of an orthorhombic $LiMnO_2$ precursor in air at an appropriate temperature.[28] However, there have been few studies on the preparation of $Li_{1.6}Mn_{1.6}O_4$ and its structural characteristics. In addition, there have been no studies on the preparation of proton-type manganese oxide derived from $Li_{1.6}Mn_{1.6}O_4$ and its ion-exchange behaviors.

In the present paper, a novel material with a composition of $MnO_2 \cdot 0.5H_2O$ was first synthesized by the acid treatment of $Li_{1.6}Mn_{1.6}O_4$. The precursor $Li_{1.6}Mn_{1.6}O_4$ was prepared by the heat treatment of $LiMnO_2$, which was prepared by hydrothermal treatment of γ-MnOOH with a LiOH solution. The structural characteristics and ion-exchange properties of $Li_{1.6}Mn_{1.6}O_4$ and $MnO_2 \cdot 0.5H_2O$ were studied by XRD, DTA-TG, IR, SEM, pH titration, and distribution coefficient measurement. This novel manganese oxide was found to have a remarkable lithium ion-sieve property and shows the largest lithium uptake from seawater among the adsorbents studied to date.

Experimental Section

Preparation of Material. The $LiMnO_2$ precursor was prepared by a hydrothermal method. Two grams of γ-MnOOH (Toyo Soda Co., Japan) was mixed with 40 mL of 4 M LiOH solution (1 M = 1 mol/L) in a Teflon-lined stainless steel vessel (50 mL) and autoclaved at 120 °C for 1 day. The precipitate was filtered, washed with deionized water, and dried at 60 °C. The obtained $LiMnO_2$ product was then heated at different temperatures: 400, 450, 500, 550, and 600 °C for 4 h in air. The Li^+ extraction was carried out batchwise by stirring 1.5 g of material with 2 L of 0.5 M HCl solution for 1 day. The acid-treated materials were filtered, washed with deionized water, and dried at 60 °C.

(22) Ooi, K.; Miyai, Y.; Katoh, S.; Abe, M. In *New Developments in Ion Exchange*, Proceedings of International Conference on Ion Exchange, ICIE, Tokyo, Japan, 1991; p 517.
(23) Miyai, Y.; Ooi, K.; Nishimura, T.; Kumamoto J. *J. Seawater Sci. Jpn.* (in Japanese) **1994**, *48*, 411.
(24) Ammundsen, B.; Jones, D. J.; Roziere, J. *Chem. Mater.* **1998**, *10*, 1680.
(25) Ammundsen, B.; Rozeire, J.; Islam, M. S. *J. Phys. Chem. B* **1997**, *101*, 8156.
(26) Ammundsen, B.; Jones, D. J.; Roziere, J.; Burns, G. R. *Chem. Mater.* **1996**, *8*, 2799.
(27) Ammundsen, B.; Burns, G. R.; Islam, M. S.; Kanoh, H.; Roziere, J. *J. Phys. Chem. B* **1999**, *103*, 5175.
(28) Tabuchi, M.; Ado, K.; Masquelier, C.; Matsubara, I.; Sakaebe, H.; Kageyama, H.; Kobayashi, H.; Kanno R.; Nakamura, O. *Solid State Ionics* **1996**, *89*, 53.

Physical Analysis. X-ray diffraction analysis was carried out using a Rigaku-type RINT 1200 X-ray diffractometer with a graphite monochromator. DTA−TG curves of materials were performed on a MAC Science thermal analyzer (system 001 200 TG-DTA) at a heating rate of 10 °C/min. Water contents of the samples were calculated from the weight loss at 400 °C. Infrared spectra were obtained by the KBr pellet method using a Perkin-Elmer System 2000 infrared spectrophotometer. SEM observations of various samples were carried out on a Hitachi-type S-2460 N scanning electron microscope.

Chemical Analysis. The adsorbent (50 mg) was dissolved in a 0.1 M hydrochloric acid solution containing hydrogen peroxide and the lithium and manganese contents were determined with a Shimadzu AA-760 atomic absorption spectrophotometer. The mean oxidation number of manganese (Z_{Mn}) was evaluated after determining the available oxygen by the standard oxalic acid method.[29]

pH Titration. A 0.10-g manganese sample was immersed in 10 mL of mixed solution (0.1 M MCl + MOH, M = Li^+, Na^+, and K^+) at varying ratios with intermittent shaking at room temperature for 1 week. After attainment of equilibrium, the lithium content in the supernatant solution was determined by atomic absorption spectrophotometry and the pH of the solution was determined with a Horiba-type pH meter, model M-13.

Distribution Coefficient (K_d) Measurement. A 0.1-g manganese oxide sample was immersed in 10 mL of solution containing 10^{-4} M of alkali metal ions at different pHs with intermittent shaking at room temperature for 1 week. The pH value was controlled using 10^{-4} M hydrochloric acid solution. After the attainment of equilibrium, the concentration of alkali metal ions in supernatant solution was determined by an atomic absorption spectrophotometer and the pH of the solution was determined. The metal ion uptake was calculated relative to the initial concentration of the solution. A K_d value was calculated using the following formula:

$$K_d\,(\mathrm{mL/g}) = \text{metal ion uptake (mg/g of material)}/\text{metal ion concentration (mg/mL of solution)}$$

Uptake of Lithium Ion from Seawater. The uptake of lithium ions from lithium-enriched seawater was carried out by stirring 100 mg of manganese oxide sample in 1 L of seawater (Li^+ concentration: 5 mg L^{-1}) for 6 days at room temperature. After attainment of equilibrium, the Li^+ ion in supernatant solution was determined by an atomic absorption spectrophotometer.

Results and Discussion

Preparation of $LiMnO_2$. Orthorhombic $LiMnO_2$ has been prepared by several methods, solid-state reaction with γ-MnOOH and LiOH·H_2O,[9,16,19] or LiCl,[30] hydrothermal reaction with γ-MnOOH and LiOH solution,[28] and a flux method in a (LiCl + LiOH) melt.[13] We adopted the hydrothermal method because a preliminary study showed that a pure $LiMnO_2$ phase with uniform crystallite size can be obtained by hydrothermal reaction at a relatively low temperature. The reaction of monoclinic-type γ-MnOOH with LiOH solution at 120 °C was an ion-exchange type replacing H^+ with Li^+ to form orthorhombic $LiMnO_2$. The preparation conditions were slightly different from those in the literature,[28] but our conditions produced few impurities, although the reaction temperature was not so high. The formula of $LiMnO_2$ was confirmed from the chemical analysis of lithium and manganese and the mean oxidation number of manganese (Z_{Mn}), which was found to be 3.03 (Table 1). The XRD patterns of the present material showed that the crystal system was identical to that of orthorhombic $LiMnO_2$ (JCPDS No. 35-0749) (Figure 2.). The relative intensity I_{120} to I_{010} was higher in our sample than that prepared at higher temperatures in the literature.[19,28] SEM observation showed that the particle shape changed from needlelike form with a length of about 3 μm and width of about 0.2 μm for starting γ-MnOOH to fine particles around 0.1 μm in size for $LiMnO_2$ (Figure 3). This shows that the Li^+ exchange of lattice hydrogen causes the destruction of hydrogen bonding, and as a result the needle particles were reduced to small particles. An infrared spectrum shows the absorption bands around 608 and 430 cm^{-1}, which were assigned to the Mn−O stretching vibrations (Figure 4).

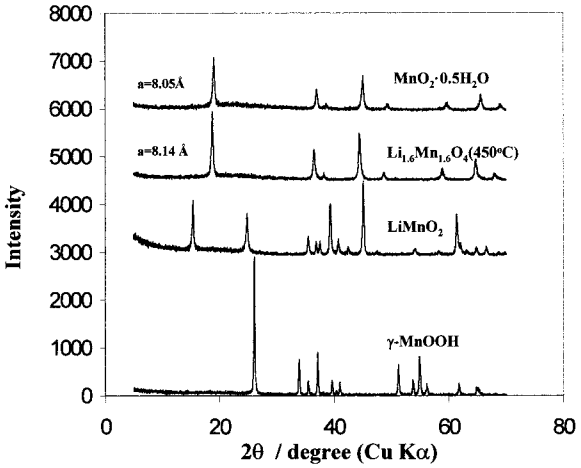

Figure 2. XRD patterns of various manganese oxides.

Table 1. Composition of $LiMnO_2$ Samples Heated at Different Temperatures and Their Delithiated Materials

starting material	heating temp. (°C)	Li/Mn	Z_{Mn}	formula
$LiMnO_2$		1.01	3.03	$Li_{1.01}MnO_{2.02}$
$LiMnO_2$	400	0.99	3.96	$Li_{1.59}Mn_{1.61}O_4$
$LiMnO_2$	450	1.00	4.00	$Li_{1.60}Mn_{1.60}O_4$

	after acid treatment			
starting material	Li/Mn	H_2O/Mn	Z_{Mn}	formula
$LiMnO_2$ (400 °C)	0.014	0.51	4.02	MnO_2·0.50H_2O·0.007Li_2O
$LiMnO_2$ (450 °C)	0.001	0.51	4.02	MnO_2·0.50H_2O·0.005Li_2O

Preparation of $Li_{1.6}Mn_{1.6}O_4$. A $Li_{1.6}Mn_{1.6}O_4$ phase was prepared by thermal treatment of $LiMnO_2$, which brings about the oxidation of manganese from trivalent to tetravalent. The DTA−TG curve of $LiMnO_2$ showed a sharp exothermic peak around 380 °C with abrupt weight gain, followed by a slow weight gain between 400 and 520 °C (Figure 5). The weight reached its maximum at 520 °C and then decreased slightly with a rise in temperature above 520 °C. The total weight gain was 8.5% at 450 °C (4 h of heating in air), which agrees well with the theoretical weight increase by the oxidation of trivalent manganese oxide to tetravalent ($LiMnO_2 + {}^1/_2O_2 \rightarrow LiMnO_{2.5}$, for which the weight increase is 8.51%). The $LiMnO_2$ was heated at different temperatures (400, 450, 500, 550, and 600 °C) for 4 h to observe the effect of heating temperature on the structure and lithium extractability. The mean oxidation numbers

(29) Japan Industrial Standard (JIS), M8233, 1969.
(30) Yang, X.; Tang, W.; Kanoh, H.; Ooi, K. *J. Mater. Chem.* **1999**, *9*, 2683.

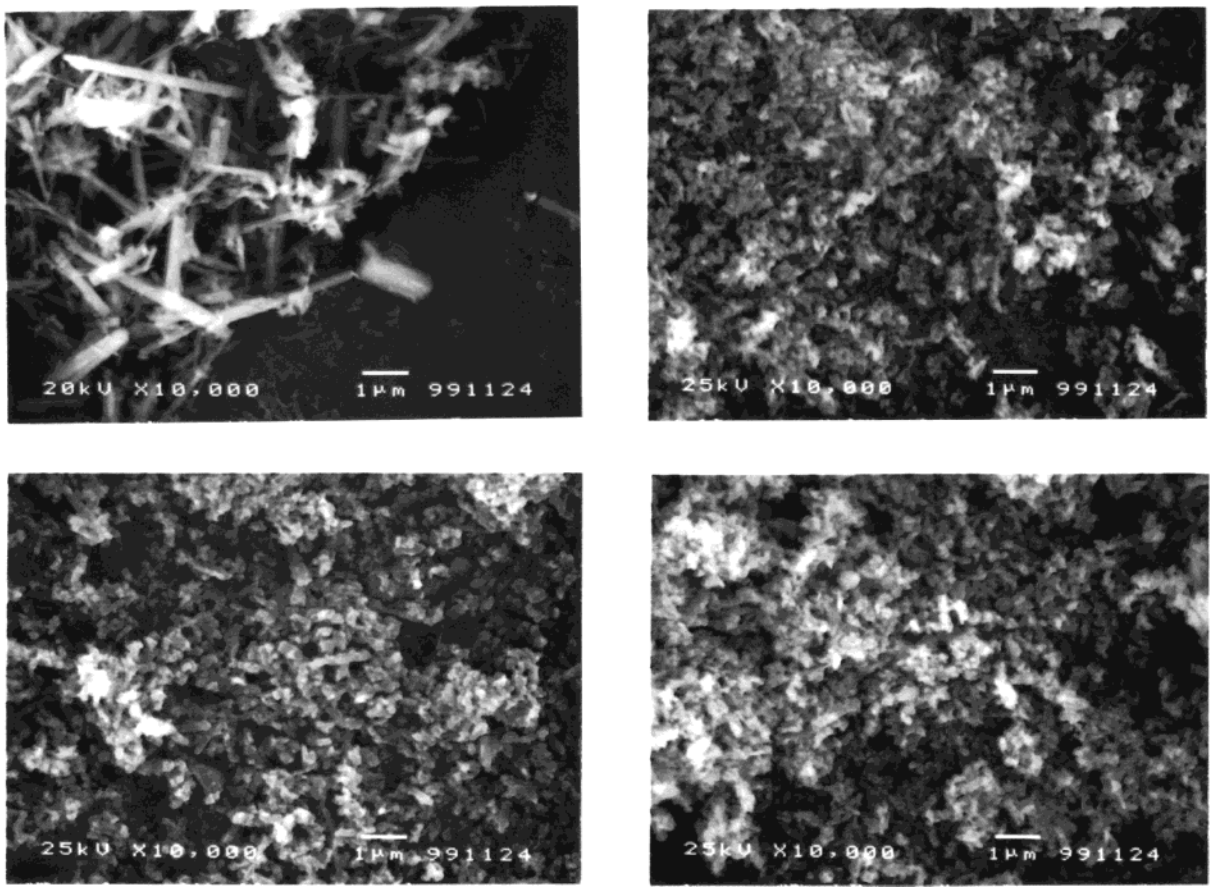

Figure 3. SEM images of γ-MnOOH (top left), $LiMnO_2$ (top right), $Li_{1.6}Mn_{1.6}O_4$ (bottom left), and $MnO_2 \cdot 0.5H_2O$ (bottom right).

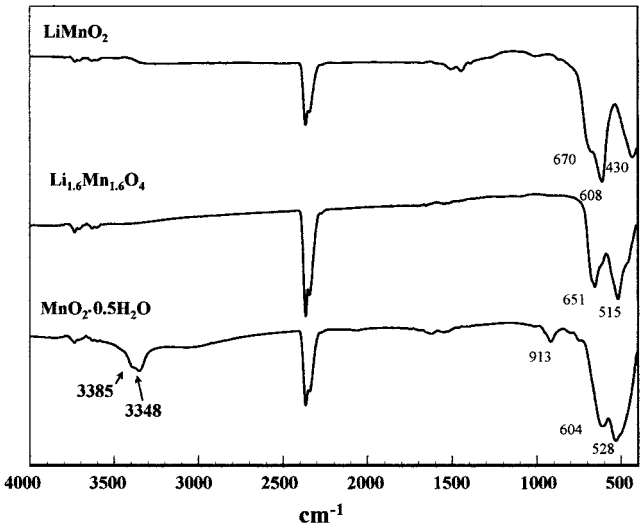

Figure 4. IR spectra of $LiMnO_2$, $Li_{1.6}Mn_{1.6}O_4$, and $MnO_2 \cdot 0.5H_2O$.

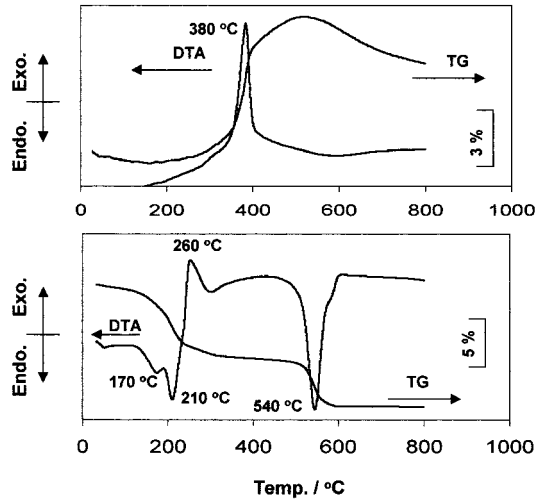

Figure 5. DTA−TG curves of $LiMnO_2$ (top) and $MnO_2 \cdot 0.5H_2O$ (bottom).

were between 3.98 and 4.00, indicating oxidation to nearly pure tetravalent manganese. The chemical composition was not so sensitive to heating temperature; all the samples had similar compositions. This suggests that the tetravalent state is stable and the chemical composition converged on $LiMnO_{2.5}$ at the cooling step, even after heating above 520 °C where the weight loss took place. SEM images of the sample heat-treated at 450 °C showed that the particle shape became clear with heating but particle growth by calcination clearly did not take place (Figure 3). The XRD patterns of the same sample is given in Figure 2. It could be indexed apparently to a face-centered cubic system with a lattice constant of 8.14 Å, but the (400) diffraction peak is relatively stronger than that of the conventional spinel-type manganese oxides. The chemical formula can be written as $Li_{1.6}Mn_{1.6}O_4$. The XRD patterns resembled each other, independent of heating temperature. All samples exhibited only the cubic phase. The lattice constants were between 8.14 and 8.15 Å. Rossouw et al.[31] have reported that $LiMnO_2$ can be decomposed into

(31) Rossouw, M. H.; Kock, A. de; Picciotto, L. A. de; Thackeray, M. M.; David, W. I. F.; Ibberson, R. M. *Mater. Res. Bull.* **1990**, *25*, 173.

a mixture of $LiMn_2O_4$ and Li_2MnO_3 by heating between 400 and 900 °C. Similar results have been obtained by Tabuchi et al.[28] and our group.[13] However, the present sample did not show apparent formation of $LiMn_2O_4$ and Li_2MnO_3. Because the crystallite size of the present sample was small compared with the other samples, the particles may have been sufficiently in contact with oxygen gas, which prevented the formation of $LiMn_2O_4$ with trivalent manganese. Because the $LiMnO_2$ is very uniform and easy to react, the heat treatment at 400 °C can oxidize all trivalent manganese in the $LiMnO_2$ to tetravalent and form $Li_{1.6}Mn_{1.6}O_4$. The total weight gain of 8.5% shows a good agreement with the theoretical weight increase of the reaction.

The composition of $Li_{1.6}Mn_{1.6}O_4$ deviated slightly from the theoretical composition of the spinel structure; the ratio of cations to anions deviates from the 3:4 of a typical spinel phase.[32] This suggests that vacancies or interstitial cations exist in the present phase. We carried out preliminary Rietveld analysis with three models: a model with excess Li in the 16c site $(Li)_{8a}[Li_{0.2}]_{16c}[Li_{0.4}Mn_{1.6}]_{16d}O_4$, a model with oxygen deficiency $(Li)_{8a}[Li_{0.5}Mn_{1.5}]_{16d}O_{3.75}$, and a model of a hexagonal lattice with cation deficiency $(Li_{0.8}\square_{0.2})_{3b}(Mn_{0.8}\square_{0.2})_{3a}O_2$. The simulation results indicate that all the models trace the XRD peaks of the heat-treated sample, but the third model (hexagonal lattice with cation deficiency) closely traces the relative intensity of the XRD peaks. This model has a layered structure (space group $R\bar{3}m$). Orthorhombic $LiMnO_2$ has a rock salt structure with a distorted cubic closed-packed oxygen anion array in which zigzag layers of lithium and manganese cations alternate with one another.[13] The orthorhombic $LiMnO_2$ precursor described in the present paper is likely to form a disordered rock salt structure such as $(Li_{1-x-y}Mn_x[\ ]_y)_{3a}(Mn_{1-w-z}Li_w[\ ]_z)_{3b}O_2$ as the result of thermal oxidation (using $R\bar{3}m$ notation). Such a structure could also be written in the cubic $Fd3m$ space group as $(Li_{2-x-y}Mn_x[\ ]_y)_{16c}(Mn_{2-w-z}Li_w[\ ]_z)_{16d}O_4$. This model would explain the unusual high intensity of the XRD peak at 44° (2θ) relative to the peak at 18.8° (2θ). In any case, a neutron diffraction analysis is needed to determine the lithium distribution. The structure of $Li_{1.6}Mn_{1.6}O_4$ is referred to as a cubic-type structure in this paper.

Preparation and Properties of MnO_2·0.5H_2O. The extractability of lithium from heat-treated samples was investigated using a 0.5 M HCl solution. The Li^+ extractability reached 99% for the lithium manganese oxides obtained at 400 and 450 °C. But the extractability decreased with heating temperature for samples obtained above 450 °C; only 87% of lithium ion could be extracted for the sample heated at 600 °C. The difference in the lithium extractability may have been due to differences in the lithium distribution in the solid depending on the heating temperature. Lithium ions can migrate between tetrahedral and octahedral sites but the lithium ions cannot be detected by XRD analysis. The dissolution of manganese during the acid treatment was <1.5% for all samples; the dissolution amount is significantly smaller that that (about 5%) for $Li_{1.33}Mn_{1.67}O_4$; this shows the higher chemical stability of the present sample.

The valences of manganese in the acid-treated samples were nearly equal to 4, independent of heating temperature of the precursor (Table 1). This shows that the extraction progresses by the Li^+/H^+ ion-exchange mechanism. The water content was determined by the weight loss following heating at 400 °C, assuming the product to be β-MnO_2 (the thermal behaviors are discussed in the next paragraph). The H_2O/Mn ratios were close to 0.50 for the samples obtained by heating below 500 °C. The ratio decreased with an increase in the heating temperature due to decreasing lithium extractability. The H_2O contents were nearly equal to the theoretical proton content calculated on the basis of Li^+/H^+ exchange reaction, suggesting that the H_2O contents corresponded to the amount of lattice hydroxyl groups formed by the exchange reaction. The XRD patterns of the acid-treated samples preserved the cubic structure with only a slight decrease of the lattice constant. The XRD of MnO_2·0.5H_2O obtained from $Li_{1.6}Mn_{1.6}O_4$ heated at 450 °C is shown in Figure 2. The pattern could be indexed to a face-centered cubic system ($Fd3m$) with lattice constant 8.05 Å. The relative intensities of the peaks were almost the same as that of the precursor $Li_{1.6}Mn_{1.6}O_4$. This indicates that the lithium extraction progressed topotactically, preserving the cubic structure. SEM images of acid-treated samples showed that the particle shapes were almost the same as the those of the precursor $Li_{1.6}Mn_{1.6}O_4$ (Figure 3). DTA−TG curves of MnO_2·0.5H_2O showed two distinct endothermic peaks around 170 and 210 °C with weight loss (Figure 5). These peaks can be ascribed to the evaporation of hydroxyl groups, which are responsible for the ion-exchange reaction. The presence of two peaks suggests two kinds of exchange sites in the MnO_2·0.5H_2O sample. The exothermic peak around 260 °C could be ascribed to the crystallization from spinel to β-MnO_2. The large endothermic peak around 540 °C with weight loss was due to the transformation from β-MnO_2 to the more stable α-Mn_2O_3 phase accompanied by dissipation of oxygen gas. IR spectra of MnO_2·0.5H_2O showed two absorption bands around 3385 and 3348 cm^{-1}, which could be assigned to stretching vibrations of hydroxyl groups in the lattice (Figure 4). Ammundsen et al.[33] reported IR spectra of both low-crystalline and high-crystalline forms of proton-exchanged $Li_{1.33}Mn_{1.67}O_4$; low-crystalline material showed only one OH stretching band at 3345 cm^{-1} while high-crystalline material showed two distinct bands at 3345 and 3440 cm^{-1}. These data are consistent with our present material. The band around 910 cm^{-1} could be assigned to the coupled lattice vibration of protons; a similar band has been observed for MnO_2·0.31H_2O.[6] The band around 1600 cm^{-1} due to the bending vibration of the hydroxyl group was not clearly observed, probably because of the restriction of the bending vibration. The absorption band between 400 and 700 cm^{-1} due to Mn−O vibrations changed slightly with extraction of lithium ions.

We can see several distinctive differences between the MnO_2·0.31H_2O derived from $Li_{1.33}Mn_{1.67}O_4$ and the present MnO_2·0.5H_2O. The present sample is highly crystalline and has markedly large proton contents.

(32) Pollert, E. *Prog. Cryst. Growth Charact.* **1984**, *9*, 263.

(33) Ammundsen, B.; Aitchison, P. B.; Burns, G. R.; Jones, D. J.; Roziere, J. *Solid State Ionics* **1997**, *97*, 269.

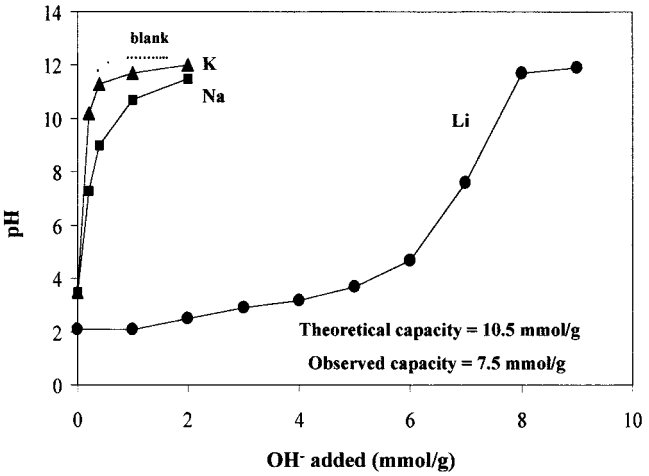

Figure 6. pH titration curves toward lithium, sodium, and potassium ions. $MnO_2 \cdot 0.5H_2O$, 0.10 g; volume, 10.0 mL; solution, 0.1 M (MCl + MOH); time: 1 week.

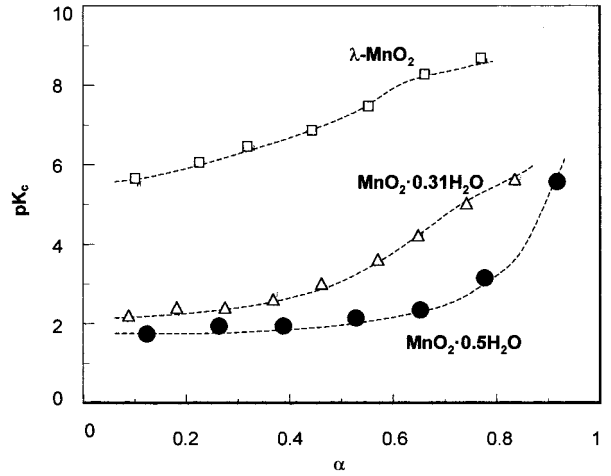

Figure 7. pK_c vs α plots calculated from Figure 6. *Data from ref 6 (for λ-MnO_2 and $MnO_2 \cdot 0.31H_2O$).

pH Titration. The pH titration curves of the $MnO_2 \cdot 0.5H_2O$ sample toward lithium, sodium, and potassium ions are shown in Figure 6. The titration curve showed monobasic acid behavior with a large exchange capacity for lithium ions but markedly low exchange capacities for sodium and potassium ions. The affinity order was K < Na ≪ Li over the entire pH range, indicating that the present sample showed a marked lithium ion-sieve property. The ion-exchange capacity reaches 7.5 mmol/g for lithium ions, which is larger than the Li^+-exchange capacity (5.4 mmol/g) of $MnO_2 \cdot 0.31H_2O$.[6] The experimentally determined exchange capacity is smaller than the theoretical capacity (10.5 mmol/g) on the basis of the chemical formula of $Li_{1.6}Mn_{1.6}O_4$. An exchange capacity so much lower than the theoretical one has been observed for conventional manganese oxide.[4−6] The neutron diffraction analysis of lithium extraction/insertion with $Li_{1.33}Mn_{1.67}O_4$ spinel has shown re-sorption only at the tetrahedral sites and not at the octahedral sites.[24] It is unlikely that the reinsertion of lithium into the octahedral sites proceeds in aqueous LiOH solution. The titration data can be analyzed on the basis of the ion-exchange mechanism as follows,

$$\overline{H^+} + Li^+ \rightleftarrows \overline{Li^+} + H^+ \qquad (1)$$

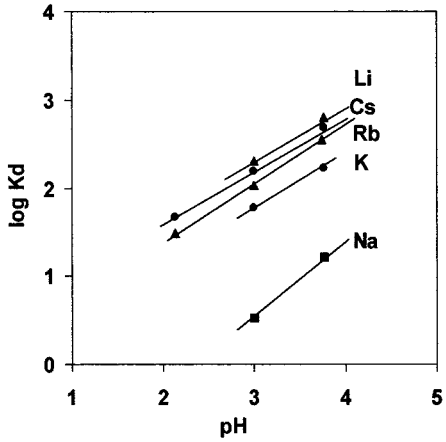

Figure 8. K_d values of alkali metal ions as a function of pH. $MnO_2 \cdot 0.5H_2O$, 0.10 g; volume, 10.0 mL; concentration, 10^{-4} M; time, 1 week.

Table 2. Lithium Uptake from Seawater with Delithiated Materials Obtained at Different Temperatures[a]

	$MnO_2 \cdot 0.5H_2O$ obtained from $Li_{1.6}Mn_{1.6}O_4$ at				
	400 °C	450 °C	500 °C	550 °C	600 °C
Li^+ uptake (mg/g)	35	37	32	32	32

[a] Adsorbent = 100 mg, volume of Li^+-enriched seawater = 1 L, concentration of Li^+ = 5 ppm (mg/L), stirring time = 6 days, and temperature = room temperature.

where the bar refers to the species in the solid phase. The equilibrium constant, K, of the above reaction can be defined as

$$K = (H^+)\,\overline{(Li^+)}/(Li^+)\overline{(H^+)}$$

$$K = \{(H^+)X_{Li}/X_H(Li^+)\}\{f_{Li}/f_H\gamma_{Li}\} \qquad (2)$$

where X_{Li} and X_H are the equivalent fractions of Li^+ and H^+ in the solid phase, respectively, f_{Li} and f_H are the activity coefficients of the Li^+ and H^+ in the solid phase, respectively, and (Li^+) and (H^+) are the activities of lithium and hydrogen ions in solution, respectively. K_c, the selectivity constant including the activity coefficient of the metal ions in solution can be evaluated from the pH titration data as follows,

$$pK_c = -\log K_c = pH - \log\{X_{Li}/X_H\} + \log[Li^+]$$

$$= pH - \log\{\alpha/(1-\alpha)\} + \log[Li^+] \qquad (3)$$

where α is the degree of neutralization. The pK_c values for $MnO_2 \cdot 0.5H_2O$ are plotted as a function of the degree of neutralization in Figure 7. The pK_c values for $MnO_2 \cdot 0.31H_2O$ and λ-MnO_2 are also plotted using the pH titration data in the literature.[6] Although the Li^+ insertion into λ-MnO_2 progresses by the redox reaction, the reaction consumes an equivalent amount of OH^- ions. Therefore, we can calculate the apparent pK_c values using the titration data. The apparent pK_c values for λ-MnO_2 are larger than those of the other two samples over the whole range of α, indicating that it has exchange sites with lower acidity than those of the other two. The intrinsic selectivity coefficient (pK_c^0) can be calculated by extrapolating the pK_c values to α = 0. Both the $MnO_2 \cdot 0.31H_2O$ and $MnO_2 \cdot 0.5H_2O$ samples have a similar pK_c^0 value of 2, indicating that the

Table 3. Comparison of Lattice Constants, Theoretical Exchange Capacities, and Lithium Uptakes of Three Adsorbents

sample	a_0 (Å)	type	theoretical exchange capacity (mmol/g)	Li^+-exchange capacity by pH titration (mmol/g)	Li uptake from Li-enriched seawater (mmol/g)
$LiMn_2O_4$	8.24	redox	5.7		
λ-MnO_2	8.03			4.5	0.16 (1.1 mg/g)
$Li_{1.33}Mn_{1.67}O_4$	8.14−8.19	ion exchange	8.5		
MnO_2·0.31H_2O	8.06			5.3	3.6 (25 mg/g)
$Li_{1.6}Mn_{1.6}O_4$	8.14	ion exchange	10.5		
MnO_2·0.5H_2O	8.05			7.5	5.3 (37 mg/g)

intrinsic acidity of the exchange sites is stronger than the acidity (about 4) of typical weak acid carboxylate. The strong acidity is advantageous for the sorption of lithium from a weakly basic solution like seawater (pH = 8.1). Because the MnO_2·0.5H_2O sample has a constant pK_c value over the wide range of the region $\alpha < 0.7$, it has a large number of uniform sites selective to lithium.

***K_d* Measurements**. The equilibrium distribution coefficients (K_d) of alkali metal ions were measured at different pH values. The selectivity sequence of alkali metal ions at micro amounts of loading was found to be in the order Na < K < Rb < Cs < Li over the entire pH range studied (Figure 8). This shows selective lithium sorption, but remarkably high K_d values were not observed for lithium ions. This may be due to the influence of incomplete Li^+ extraction during acid treatment. A small amount of Li^+ dissolution from the solid causes a marked decrease of the K_d values. The slope of d log K_d/d pH of all alkali metal ions was lower than the expected ideal 1:1 ion-exchange reaction (slope 1). The low slope might be due to the self-dissociation of protons on the surface sites at higher pH ranges. A low slope has been reported for the K_d values of alkali metal ions except lithium ions on λ-MnO_2, the selectivity sequence being Na < K < Rb < Cs ≪ Li over the entire pH range.

Lithium Uptake from Li-Enriched Seawater. Lithium uptake from Li-enriched seawater was studied using delithiated materials (Table 2). A maximum uptake of 37 mg/g (5.3 mmol/g) was observed for the MnO_2·0.5H_2O sample prepared by acid treatment of $Li_{1.6}Mn_{1.6}O_4$ heated at 450 °C. The large lithium uptake of the present sample is due to the availability of strongly acidic sites in MnO_2·0.5H_2O samples as evidenced from the pH titration curve toward lithium ions.

Comparison of λ-MnO_2, MnO_2·0.31H_2O, and MnO_2·0.5H_2O. A comparison was made of the three adsorbents (Table 3). The lattice constants, a_0 of $LiMn_2O_4$, $Li_{1.33}Mn_{1.67}O_4$, and $Li_{1.6}Mn_{1.6}O_4$ were found to vary slightly, that is, 8.24, 8.14−8.19, and 8.14 Å, respectively. The lattice constant of $Li_{1.33}Mn_{1.67}O_4$ varies depending on the preparation method. All delithiated materials had almost the same lattice constant (a_0 = 8.05 Å). The exchange capacity of MnO_2·0.5H_2O toward Li^+ was higher than those reported for λ-MnO_2 and MnO_2·0.31H_2O. The present material, MnO_2·0.5H_2O, exhibited high lithium uptake from Li-enriched seawater as compared to λ-MnO_2 and MnO_2·0.31H_2O.[22,23]

Conclusion

A novel manganese oxide having the formula MnO_2·0.5H_2O was synthesized from $Li_{1.6}Mn_{1.6}O_4$. The ion-exchange behavior of MnO_2·0.5H_2O was found to be different from other manganese oxides λ-MnO_2 and MnO_2·0.31H_2O derived from $LiMn_2O_4$ and $Li_{1.33}Mn_{1.67}O_4$, respectively. The present material is the most promising adsorbent for lithium in seawater because of its large sorptive capacity and high chemical stability.

CM0000191